Applied Mathematics & Information Sciences
An International Journal

http://dx.doi.org/10.18576/amis/100423

Comparison of Wavelet and Shearlet Transforms for Medical Images

Hülya Kodal Sevindir[1,*] *and Cüneyt Yazıcı*[2,*].

[1] Department of Mathematics, University of Kocaeli, Umuttepe Campus, 41380, Kocaeli, Turkey.
[2] Department of Mathematics Education, University of Kocaeli, Umuttepe Campus, 41380, Kocaeli, Turkey

Received: 25 Dec. 2014, Revised: 22 May 2016, Accepted: 23 May 2016
Published online: 1 Jul. 2016

Abstract: Incomplete data is an important problem in the data analysis of all areas. There have been a number of applications related to inpainting problem which are intriguing. In these papers mathematical theory of shearlet and wavelet transforms related to inpainting problem are studied and numerical application results are compared, and several inpainting methods are applied to images with vertical, square and random masking. In one of these studies the suggested undone problems includes applying circular masking. In this paper following this suggestion, firstly circular masking with arbitrary radius is developed and applied to images, then shearlet and wavelet transforms are applied to images with circular masking to recover the images. Numerical results show that shearlets are able to inpaint larger gaps than wavelets in the circular masking case.

Keywords: inpainting, shearlet, wavelet, circular masking, iterative thresholding

1 Introduction

In almost any research performed, there is the potential for missing or incomplete data. Incomplete or missing data can occur for many reasons. Incomplete data are a common occurrence and can have a significant effect on the conclusions that can be drawn from the data. It can reduce the representativeness of the image and can therefore distort inferences about the images. If it is possible, preventing data from missingness before the actual data gathering takes place is useful. However, this technique may not be practical especially working with medical data. In situations where incomplete data are likely to occur, the researcher is often advised to plan to use robust methods of data analysis.

Repairing gaps in images is a significant inverse problem in both the analog and the digital area with many applications. Removal of scratches in old photos, removal of overlaid text or graphics, filling-in missing blocks in unreliably transmitted images, scaling-up images, predicting values in images for better compression, and more, are all examples of inpainting. In many cases medical technicians state that they may be missing significant data during the recording as well. Inpainting would be a better choice when repeating the process may not be possible for one reason or another. In recent years this topic attracted much interest, and many contributions have been proposed for the solution of this interpolation problem [2,3,5,9,10,12]. Two recent papers related to inpainting problem are interesting [2,3]. In [2] mathematical theory of shearlet and wavelet transforms related to inpainting problem are studied and numerical application results are compared. In [3] several inpainting methods applied to images with different maskings. In [2] one of the suggested undone problems includes applying circular masking.

In this paper, our contribution is two-fold. We will present a circular masking of arbitrary radius. Then we will describe the missing traces recovery as an image inpainting problem using wavelets and shearlets with iterative thresholding.

The organization of the paper is as follows: In Section 2 we introduce the basics of wavelet and shearlet transforms briefly. In Section 3 we outline a few methods of inpainting problem in the literature. In Section 4 we give algorithms of circular masking and wavelet/shearlet inpainting problem. In the same section we apply the circular masking to sample images and numerically test shearlet-based inpainting algorithm against wavelet inpainting method to the masked images.

* Corresponding author e-mail: hkodal@kocaeli.edu.tr, cuneyt.yazici@kocaeli.edu.tr

© 2016 NSP
Natural Sciences Publishing Cor.

2 Basics of wavelet and shearlet transforms

2.1 Wavelet transform

For two dimensional wavelets let $\psi \in Ł^2(R^2)$. Let the continuous affine systems of $Ł^2(R^2)$ be defined as $\psi_{M,t} = T_t D_M^{-1}\psi = |detM|^{\frac{1}{2}}\psi(M(.-t)) : (M,t) \in GxR^2$. Here G is a subset of $GL_2(R)$, the group of d-dimensional invertible matrices, and D_M is the dilation operator on $Ł^2(R^2)$, defined by $D_M\psi(x) = |detM|^{\frac{-1}{2}}\psi(M^{-1}x), M \in GL_2(R)$. T_t is the translation operator on $Ł^2(R^2)$, defined by $T_t\psi(x) = \psi(x-t), t \in R^2$. Any $f \in Ł^2(R^2)$ can be recovered from its coefficients $(\langle f, \psi_{M,t}\rangle)_{M,t}$. So, one needs to determine conditions on ψ. For this, define a group structure as $(M,t).(M^{'},t^{'}) = (MM^{'}, t+Mt^{'})$. The resulting group, typically denoted by A_2, is the so-called affine group on R^2. Reproducibility of functions in $L^2(R^2)$ is available as well [1,7].

Theorem: Let d_μ be a left-invariant Haar measure on $G \subset GL_2(R)$, and d_λ be a left Haar measure of A_2. Moreover, suppose that $\psi \in Ł^2(R^2)$ satisfies the admissibility condition $\int_G |\hat{\psi}(M^T\xi)|^2|detM|d_\mu(M) = 1$. Then any function $f \in Ł^2(R^2)$ can be recovered via the reproducing formula $f = \int_A \langle f, \psi_{M,t}\rangle \psi_{M,t} d\lambda(M,t)$ interpreted weakly [4]. When the conditions of the above theorem are satisfied, $\psi \in Ł^2(R^2)$ is called a continuous wavelet. The Continuous Wavelet Transform is defined to be the mapping. $L^2(R^2) \ni f \to W_\psi f(M,t) = \langle f, \psi_{M,t}\rangle, (M,t) \in A_2$.

2.2 Shearlet transform

Shearlets has emerged in recent years with many successful applications; some related work can be listed as [6,8,11]. The scaling operator is required to generate waveforms with anisotropic support. We utilize the family of dilation operators $D_{A_a}, a > 0$, based on parabolic scaling matrices A_a of the form $(A_a) = \begin{pmatrix} a & 0 \\ 0 & \sqrt{a} \end{pmatrix}$ where the dilation operator is given like wavelets. An orthogonal transformation is to change the orientations of the waveforms. As orthogonal transformation, we choose the shearing operator $D_{S_s}, s \in R$ where the shearing matrix S_s is given by $(S_s) = \begin{pmatrix} 1 & s \\ 0 & 1 \end{pmatrix}$. The shearing matrix parameterizes the orientations using the variable s associated with the slopes rather than the angles, and has the advantage of leaving the integer lattice invariant, provided s is an integer. Finally, for the translation operator we use the standard operator T_t given by wavelets. Combining these three operators, we define continuous shearlet systems as follows [1]. For $\psi \in Ł^2(R^2)$, the continuous shearlet system $SH(\psi)$ is defined by $SH(\psi) = \{\psi_{a,s,t} = T_t D_{A_a} D_{S_s}\psi : a > 0, s \in R, t \in R^2\}$. Let S denote the Shearlet group and define $(a,s,t).(a',s',t') = (aa', s+s'\sqrt{a}, t+S_sA_at')$ group multiplication on R^+xRxR^2. Letting the unitary representation $\sigma : S \to U(L^2(R^2))$ be defined by $\sigma(a,s,t)\psi = T_t D_{A_a} D_{S_s}\psi$, where $U(L^2(R^2))$ denotes the group of unitary operators on $L^2(R^2)$ a continuous shearlet system $SH(\psi)$ can be written as $SH(\psi) = \{\sigma(a,s,t)\psi : (a,s,t) \in Ł^2(R^2)\}$.

3 Inpainting

The main inpainting methods are primarily divided into three categories: sparsity-based, variational, and patch-based. Sparsity-based methods involve a combination of harmonic analysis with convex optimization (see, for example, [9,10,13]). Recently the compressed sensing methodology, namely exact recovery of sparse or sparsified data from highly incomplete linear nonadaptive measurements by minimization or thresholding, has been very effectively applied to this problem. The pioneering paper is [9] which uses curvelets as sparsifying system for inpainting. The minimization task in [9] is $x^* = x_1^* + x_2^*, (x_1^*, x_2^*) = \arg\min_{x_1,x_2} \|\Phi_1^* x_1\|_1 + \|\Phi_2^* x_2\|_1 + \lambda\|P_M(x^0 - x_1x_n)\|_2^2 + \gamma TV\{x_2\}$ where Φ_1 is a parseval frame consisting of parabolic molecules, Φ_2 is an oscillatory Parseval frame like DCT, Gabor, wavelet packets, and λ, γ are parameters. The algorithm used is based on the block-coordinate relaxation method. Also, some work has been done to compare variational approaches with those built on ℓ_1 minimization [14,15]. It also prohibits a deep understanding of why directional representation systems such as shearlets outperform wavelets when inpainting images strongly governed by curvilinear structures such as seismic images. Variational methods have been used on a number of papers in image processing literature. A few of these are [16,17,18,19] The main idea of variational-based inpainting is that information is propagated from the boundary of the holes along isophotes (edges) in the image to fill them in. Many of the methods are inspired by real physical processes, like diffusion, osmosis, and uid dynamics. In patch based or exemplar based inpainting, information is also propagated from the edge(s) of the missing data inward. However, in contrast to the variational approaches, the hole is iteratively filled using patches or averages of patches from other parts of the image [3]. Some examples of exemplar based inpainting are [20,21,22,23].

Compressed sensing techniques in combination with both wavelet and directional representation systems have been very effectively applied to the problem of image inpainting recently. A mathematical analysis of these techniques which reveals the underlying geometrical content is presented in [2]. In the same paper, the first comprehensive analysis is provided in the continuum

© 2016 NSP
Natural Sciences Publishing Cor.

domain utilizing the novel concept of clustered sparsity, which besides leading to asymptotic error bounds also makes the superior behavior of directional representation systems over wavelets precise. The computational method in our paper also follows this line. In our study we use wavelet and shearlet transforms to circular masked images. To our best knowledge this is the first time shearlet based inpainting is applied to circular masked images.

4 Numerical results

In this study we want to present the results of our approach with four different data sets. The first two are well known 512*x*512 Lena and Peppers images shown in Fig. 1 and Fig. 2. The other two images, obtained through Medical Schools Hospital at Kocaeli University in Turkey, are vessel contour image shown in Fig. 3 and chest X-ray image in Fig. 4.

Fig. 1: 512x512 Lena

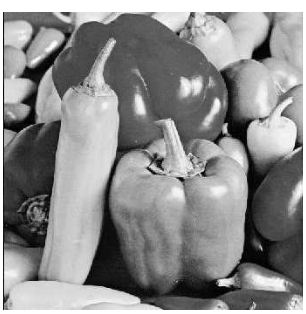

Fig. 2: 512x512 Peppers

Circular masking code is written in Matlab for arbitrary radius. A circular masking is shown in Figure 5 with radius 10 pixels. Obtained circular masking is

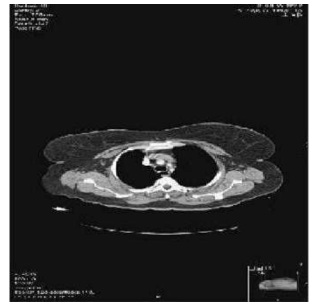

Fig. 3: Vessel contour image

Fig. 4: Chest X-Ray image.

applied to the all four images, see Figures 6(b), 7(b), 8(b) and 9(b) covering in total 22% of the images. Masked images are inpainted by wavelets shown in Figures 6(c), 7(c), 8(c), and 9(c) and shearlets in Figures 6(d), 7(d), 8(d), and 9(d). For shearlets, some part of the shearlet program codes are obtained at the shearlet web site www.shearlet.org.

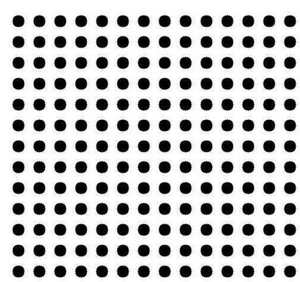

Fig. 5: Circular Masking with radius 10 pixels.

The algorithms for both circular masking and wavelet/shearlet inpainting problem are shown in Fig. 10 and Fig. 11, respectively.

© 2016 NSP
Natural Sciences Publishing Cor.

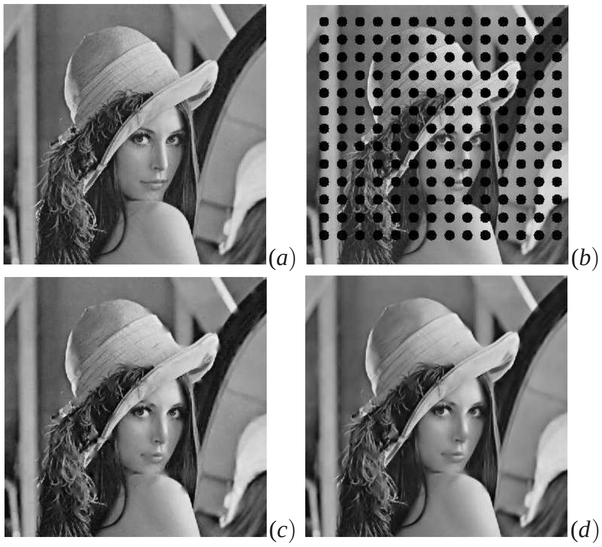

Fig. 6: (a) Lena; (b) Lena after circular masking; (c) inpainting of Lena with wavelet transformation; (d) inpainting of Lena with shearlet transformation.

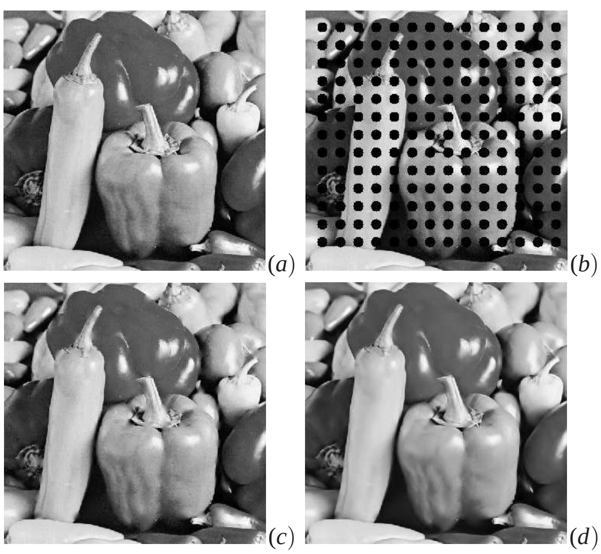

Fig. 7: (a) Peppers; (b) Peppers after circular masking; (c) inpainting with wavelets; (d) inpainting with shearlets.

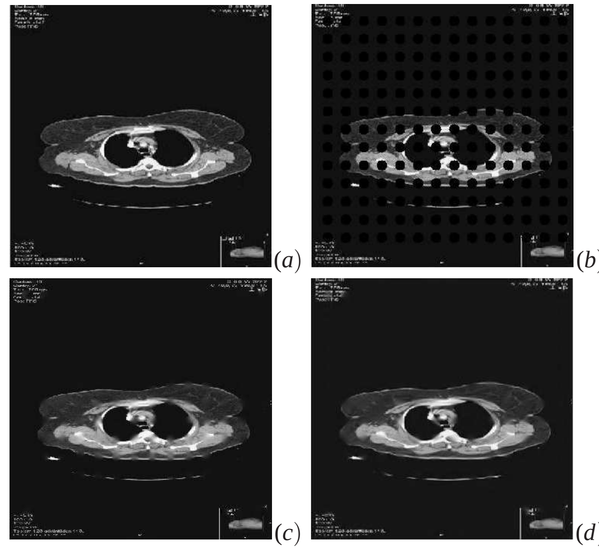

Fig. 8: (a) Vessel contour image; (b) Vessel contour after circular masking; (c) inpainting with wavelets; (d) inpainting with shearlets.

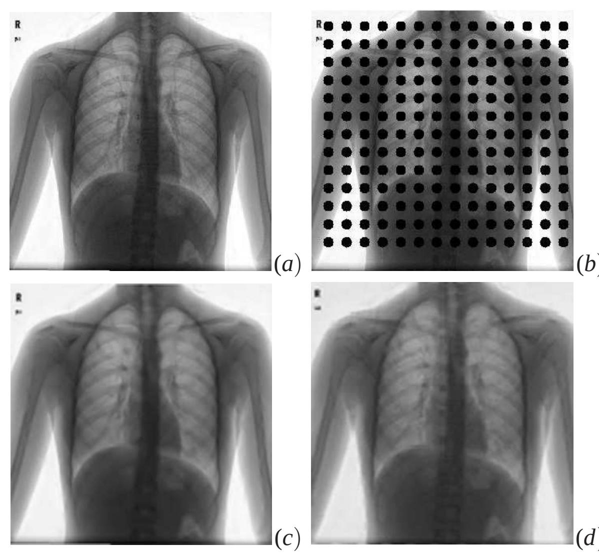

Fig. 9: (a) Chest X-Ray; (b) Chest X-Ray after circular masking; (c) inpainting with wavelets; (d) inpainting with shearlets.

The phrase peak signal-to-noise ratio, often abbreviated PSNR, is an engineering term for the ratio between the maximum possible power of a signal and the power of corrupting noise that affects the fidelity of its representation. Because many signals have a very wide dynamic range, PSNR is usually expressed in terms of the logarithmic decibel scale. As a performance measure, computation of PSNR values can be calculated as $PSNR = 10\log_{10}(\frac{MAX_I^2}{MSE})$. Here, MAX_I is the maximum possible pixel value of the image. The mean squared error (MSE) which for two mn monochrome images I and K where one of the images is considered a noisy approximation of the other is defined as: $MSE = \frac{1}{nm}\sum_{i=0}^{m-1}\sum_{j=0}^{n-1}(I(i,j)-K(i,j))^2$.

© 2016 NSP
Natural Sciences Publishing Cor.

Parameters:

- Radius parameter h.
- Image size parameters.
- Zero matrix with the same size as the image matrix.
- Step size.

Algoritm:

1. Obtaining circular mask with radius h.
2. Flooring circular masks with radius h in the whole image.

Output:

- Circular mask matrix.

Fig. 10: Cicular mask algorithm.

Parameters:

- Image.
- Circular mask.
- Iteration parameter.
- Wavelet /Shearlet transformation filters.

Algoritm:

1. Applying circular mask algorithm to image.
2. Determining threshold value using iterative thresholding.
3. Obtaining image with wavelet/shearlet transformation.
4. Calculating PSNR values.

Output:

- Masked Image.
- Inpainted image.
- PSNR values.

Fig. 11: Inpainting algorithm with wavelet /shearlet transformation.

Table 1: Comparison of the PSNR values for the images for both wavelet and shearlet inpainting methods.

Images	Wavelet transform	Shearlet transform
Lena	29.9672dB	31.6670dB
Pepers	29.4306dB	30.4066dB
Vessel contour	30.1067dB	31.0688dB
Chest X-Ray	35.0087dB	37.7624dB

In Table 1 PSNR values are calculated for each image and compared for both methods applied with 10 pixel radius masking. According to the PSNR values shearlet transform gives better results in all four cases recovering the images when applied circular masking. With the masking applied in total a little more than 22% of the images are circularly blocked. Figure 12 below shows graph of compared PSNR values of the images for both wavelet and shearlet inpainting methods with radii 8, 10, 12 and 15 pixels of circle maskings. Our numerical results show that both wavelet and shearlet can tolerate if the diameter size of the circle is less than 34 pixels. In each case shearlets outperform wavelets.

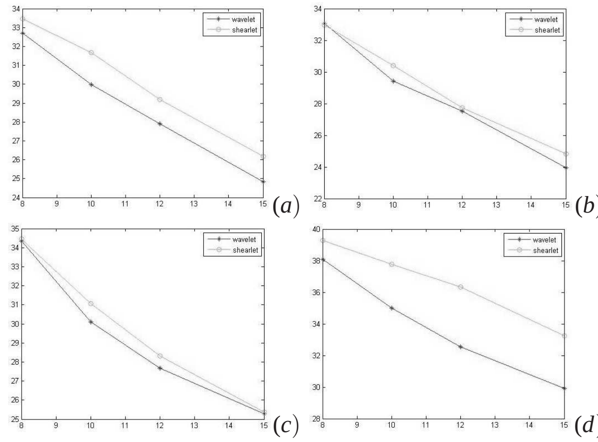

Fig. 12: Comparison of the PSNR values of the images for both wavelet and shearlet inpainting methods with radii 8, 10, 12 and 15 pixels of circle maskings. (a) Lena; (b) Peppers; (c) Vessel contour; (d) Chest X-ray.

5 Conclusions

In this paper we develop a circular masking algorithm for arbitrary radius, and apply wavelet and shearlet image inpainting to recover circular masked data including two medical images with 22% of the test data masked. The provided results show the excellent performance of shearlet inpainting, if the radius is less than 17. Obviously this depends heavily on the structure of the missing elements. When the radius is more than 17, we observed that both methods are not able to inpaint properly.

Conflict of Interests

The authors declare that there is no conflict of interests regarding the publication of this paper.

Acknowledgement

The authors wish to thank Dr.Wang Q. Lim for his valuable comments.

References

[1] G. Kutyniok and D. Labate, Shearlets: Multiscale Analysis for Multivariate Data, Birkhauser, 1-346 2012.

[2] E. J. King, G. Kutyniok, X. Zhuang, Analysis of Inpainting via Clustered Sparsity and Microlocal Analysis, Journal of Mathematical Imaging and Vision **48(2)**, 205-234 (2014).

[3] E. J. King, G. Kutyniok, W. Q. Lim, Image Inpainting: Theoretical Analysis and Comparison of Algorithms, SPIE Proceedings, **8858** (2013).

© 2016 NSP
Natural Sciences Publishing Cor.

[4] A. Grossmann, J. Morlet, T. Paul, Transforms associated to square integrable group representations I: General Results, J. Math. Phys., **26**, 24732479 (1985).
[5] R. Gomathi and A. V. A. Kumar, A Multiresolution Image Completion Algorithm for Compressing Digital Color Images, Journal of Applied Mathematics, **757318** (2014).
[6] H. Kodal Sevindir and C. Yazici An image denoising application using shearlets, AIP Conf. Proc., **1558**, 2478-2482 (2013).
[7] J. Yinpeng, A. Elsa, L. Andrew, Wavelets in Medical Image Processing: De-noising, Segmentation, and Registration Handbook of Biomedical Image Analysis International Topics in Biomedical Engineering, 305-358 (2005).
[8] G. R. Easley and D. Labate, Image Processing using Shearlets, Applied and Numerical Harmonic Analysis, 283-325 (2012).
[9] M. Elad, J.-L. Starck, P. Querre, D. L. Donoho, Simultaneous cartoon and texture image inpainting using morphological component analysis (MCA), Appl. Comput. Harmon. Anal., **19**, 340-358 (2005).
[10] J. F. Cai, R. H. Cha, Z. Shen, Simultaneous cartoon and texture inpainting, Inverse Probl. Imag., **4**, 379 395 (2010).
[11] P. Grohs and G. Kutyniok, Parabolic molecules, Found. Comput. Math., **14/2**, 299-337 (2014).
[12] E. J. King, G. Kutyniok, X. Zhuang, Analysis of data separation and recovery problems using clustered sparsity, SPIE Proceedings: Wavelets and Sparsity XIV, **8138**, (2011).
[13] B. Dong, H. Ji, J. Li, Z. Shen, Y. Xu, Wavelet frame based blind image inpainting, Appl. Comput. Harmon. Anal., **32**, 268279 (2012).
[14] . F. Cai, B. Dong, S. Osher, Z. Shen, Image restoration: Total variation, wavelet frames, and beyond, J. Amer. Math. Soc., **25**, 1033-1089 (2012).
[15] Y. Meyer, Oscillating patterns in image processing and nonlinear evolution equations, University Lecture Series, American Mathematical Society, Providence, RI, 2001.
[16] C. Ballester, M. Bertalmio, V. Caselles, G. Sapiro, J. Verdera, Filling-in by joint interpolation of vector fields and gray levels, IEEE Trans. Image Process., **10**, 1200-1211 (2001).
[17] M. Bertalmio, A.L. Bertozzi, G. Sapiro, Navier-stokes, Fluid dynamics, and image and video inpainting, Proceedings of the 2001 IEEE Computer Society Conference on Computer Vision and Pattern Recognition, IEEE, 355-362 (2001).
[18] M. Bertalmio, G. Sapiro, V. Caselles, C. Ballester, Image inpainting, Proceedings of SIGGRAPH 2000, New Orleans, 417-424 (2000).
[19] T. F. Chan, J. Shen, Mathematical models for local nontexture inpaintings, SIAM J. Appl. Math., **62**, 1019-1043 (2001).
[20] A. Criminisi, P. Perez, K. Toyama, Region filling and object removal by exemplar-based image inpainting, IEEE Trans. Image Process., **13**, 1200-1212 (2004).
[21] L. Lorenzi, F. Melgani, G Mercier, Inpainting strategies for reconstruction of missing data in vhr images, IEEE Geoscience and Remote Sensing Letters 8, **5**, 914-918 (2011).
[22] A. Wong, J. Orchard, A nonlocal-means approach to exemplar-based inpainting, 15th IEEE International Conference on Image Processing, IEEE, 2600-2603 (2008).
[23] A. Buades, B. Coll, J. M. Morel, A review of image denoising algorithms, with a new one, Multiscale Modeling and Simulation (SIAM interdisciplinary journal), **4**, 490-530 (2006).

Hülya Kodal Sevindir received the PhD degree in Mathematics at the City University of New York, U.S.A. She is currently an Assistant Professor of Mathematics at Kocaeli University. Her research interests are in the areas of applied mathematics including the the applied harmonic analysis, wavelet theory, shearlet theory, applied functional analysis, numerical analysis, algorithm analysis, applied linear algebra.

Cüneyt Yazıcı received the PhD degree in Mathematics at the Kocaeli University of Kocaeli, Turkey. He is currently an Assistant Professor of Mathematics Education at Kocaeli University. His research interests are in the areas of applied mathematics including the applied harmonic analysis, wavelet theory, shearlet theory, applied functional analysis, numerical analysis, algorithm analysis, applied linear algebra